Turbine Vane Ceramic Endwall

Charles W. Hayes[*]
Pratt & Whitney Aircraft Division, United Aircraft Corporation, East Hartford, Conn.
and
Captain Donald Zabierek[†]
Air Force Aero-Propulsion Laboratory, Wright-Patterson Air Force Base, Ohio

The feasibility of using ceramic material for turbine vane platforms was demonstrated under Air Force sponsorship (Contract F33615-73-C-2066). The high temperature capability of this material permits operation with reduced coolant flow, providing a turbine efficiency improvement which can be translated into improved engine performance. In the demonstration, platforms were fabricated from hot-pressed silicone nitride and tested at elevated temperature in a cascade of transpiration-cooled turbine vanes representative of advanced engine concepts. The platforms successfully completed ten hours of steady-state endurance testing with surface temperatures in excess of 2000°F with no damage. Subsequent thermal cyclic testing resulted in cracking near the trailing edge on two of the platforms, while the third remained intact. Preliminary analysis of the results indicates that relatively minor design modifications should solve this problem.

Introduction

THE trends for the development of advanced gas turbine engines show substantial increases in turbine temperatures. This trend is stimulated by the improvement in efficiency available with the higher temperatures, but the growth in temperature continues to be limited by the capabilities of existing turbine materials. Experimental gas turbine engines, and even some engines in service, operate with gas temperatures well above the temperature capability of turbine alloys, requiring significant coolant flows to maintain tolerable metal temperatures. For example, the coolant flow required for a typical stage of vane platforms amounts to approximately 2–4% of the total engine airflow and imposes an efficiency penalty of about 0.35–0.70 percentage point.

Efforts to recoup this performance loss have been directed toward a search for better materials with higher temperature capability, and toward the development of more effective cooling techniques to reduce the coolant flow requirement. In the search for better materials, ceramics have frequently been mentioned because they retain their tensile strength at temperatures well above 2000°F. This capability offers substantial benefits to the engine. First, the higher temperature capability of the ceramic relative to advanced nickel superalloys conventionally used in turbine endwalls, permits approximately a 50% reduction in the endwall cooling requirement and, in some instances, permits the endwalls to be operated without cooling. This reduction amounts to a 1.3–1.5% reduction in the total turbine cooling airflow requirement. These cooling flow reductions can be translated into improved turbine and overall cycle efficiency which, in turn, can be utilized to increase the fan work. The result is an increase in the bypass ratio, a reduction in the engine core size, and an increase in the engine thrust-to-weight ratio. An improvement in thrust specific fuel consumption is also obtained. The improvement in turbine efficiency amounts to 0.4–0.5%, while the improvement in thrust specific fuel consumption amounts to 0.5–1.0%. Thrust-to-weight ratio improvements are expected to amount to 1.3–1.5%.

The development of ceramic components for gas turbine engines has been slow, however, because the extreme brittleness of most ceramics produces excessive stresses when the materials are subjected to typical gas turbine engine thermal gradients. Recently, the continuing development of ceramic technology, coupled with the growing pressure for high temperature turbine materials, reached the level where demonstration testing of a ceramic material in a turbine application was warranted, both to determine the inherent feasibility of ceramics in gas turbine engines, and to provide direction for future development. In response to this need, the Air Force Aero-Propulsion Laboratory sponsored a program at Pratt & Whitney Aircraft under Contract F33615-73-C-2066 to test ceramic platforms (or endwalls) in a vane cascade at typical advanced turbine temperatures. The work involved selection of a suitable ceramic material; selection of design criteria for temperature limits, stress, creep, and cyclic life; design and fabrication of the platforms; and testing to map the surface temperatures of the platforms and to assess their steady-state and thermal cycle endurance capabilities.

Material Selection and Procurement

The ceramic material used in the program was selected on the basis of availability, reliability, and past experience, as well as on the basis of physical and chemical properties. Most important of the physical properties, of course, was high strength at the anticipated operating

Table 1 Quality control tests on hp silicon nitride billet

Test	Criterion	Result
Density	3.2 gm/cu cm minimum	3.26 gm/cu cm
Radiography	Material variations at 1% sensitivity	No variations
Ultrasonic	Delaminations, voids, and inclusions	None
Modulus of rupture	4 point bend strength	
	100 ksi at 20°C	108 ksi
	32 ksi at 1300°C	41 ksi
Thermal shock	Liquid metal quench resistance of $^1/_8$ bar; min $\Delta T = 775$°C	820°C
Chemistry	Emission spectrograph of prior billet	Consistent
Microstructure	Grain size and morphology of prior billet	Consistent

---

Received August 26, 1974.

Index categories: Airbreathing Propulsion, Subsonic and Supersonic; Thermal Modeling and Experimental Thermal Simulation.

[*] Assistant Project Engineer.

[†] Project Engineer.

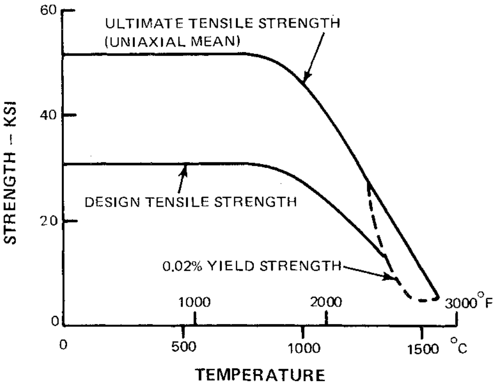

Fig. 1 Ultimate, 0.2% yield, and design stress characteristics for hot-pressed silicon nitride.

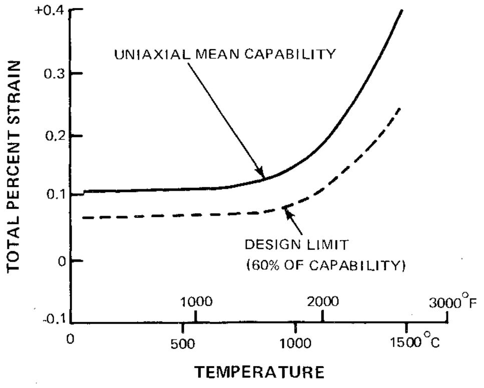

Fig. 3 Ultimate and design transient strain characteristics for hot-pressed silicon nitride.

temperatures. On the basis of these criteria, two materials, silicon nitride and silicon carbide, appeared promising. Silicon nitride was selected because it had been available in a fine grained, reliable form for a longer period than silicon carbide and because the available data indicated that silicon nitride would provide better thermal shock resistance. Thermal shock resistance was considered to be particularly important since the major stresses in the platform were expected to result from thermal gradients. The material was obtained in hot pressed rather than sintered form because of the considerably better mechanical strength at temperatures below 2000°F offered by the hot pressed material. The higher cost of the hot pressed material was not considered to be important for this demonstration test.

On the basis of this evluation, hot-pressed (HP) silicon nitride, designated Norton NC 132, was procured in the form of a single 6 × 6 × 1½ in. billet. The billet was subjected to radiographic and ultrasonic inspection using the pulse-echo method. A section machined from the center was tested for flexural strength and thermal shock resistance. In addition, chemistry and microstructure were determined by conventional techniques, and the results were compared with historical data for similar material to establish consistency. The results of the acceptance tests are shown in Table 1 and indicate that the material met all acceptance criteria.

Design Criteria

Design criteria were established for tensile stress and temperature, creep stress, and thermal stress. Generally, the design limits were set at 60% of the published capability of the material to provide a safety margin in view of the limited experience with ceramics in this application. Ultimate tensile stress data for silicon nitride are shown in Fig. 1 together with the design stress curve at 60% of the ultimate strength for each temperature. The uniaxial ultimate tensile strength was used instead of the flexural strength, to ensure a conservative design since the uniaxial strength is known to be considerably lower than the flexural strength. The data show that the strength begins to decrease rapidly above 2000°F and that plastic deformation occurs above 2400°F. On this basis, as well as considerations of creep strength and oxidation, a maximum design temperature limit of 2400°F was established. At this temperature, the maximum design stress is 18 ksi.

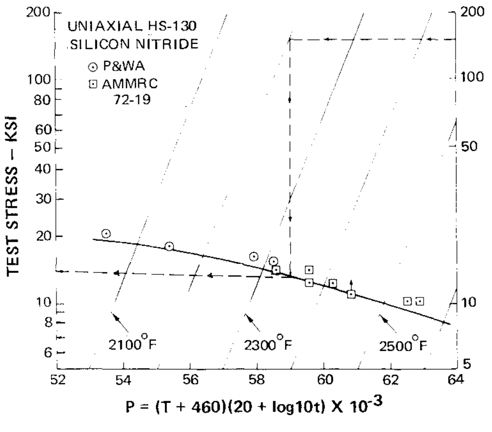

Fig. 2 Creep property extrapolation for hot-pressed silicon nitride.

Only limited creep stress information was available, but the data were available from Pratt & Whitney Aircraft and from AMMRC Report 72-19 were correlated by means of the Larson-Miller plot shown in Fig. 2. These data indicated that creep failure could be expected at 150 hr at an average temperature of 2200°F with a creep stress of approximately 14 ksi. Using the 60% safety margin criterion, the maximum allowable creep stress is 8.4 ksi. No limits were set on allowable creep strain.

Thermal stress is probably the principal stress in a vane platform, but it is also the stress for which the least data were available for ceramic materials. Data were available relating the thermal shock capability to the ultimate tensile strength for single shocks, but no data were available describing the effects of repetitive thermal shocks below the level that would cause immediate failure. Consequently, a limited amount of supplementary testing was conducted to explore the thermal fatigue characteristics of silicon nitride ceramic. Testing consisted of thermal cycling samples in a fluidized thermal fatigue bed to temperatures exceeding 2000°F. These results indicated that thermal cyclic lives in excess of 1000 cycles could be expected if the thermal strain remained below 60% of the ultimate tensile strain. This limit is shown in Fig. 3.

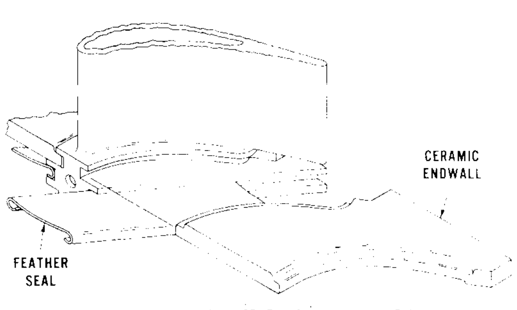

Fig. 4 Ceramic endwall design assembly concept.

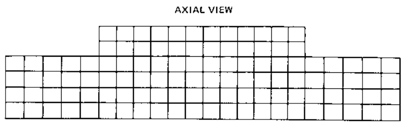

Fig. 5 **Axial view of ceramic endwall computer analysis break up.**

Design

The design effort involved establishing a mechanical design that was compatible with advanced engine turbine vane concepts, and then conducting a detailed thermal stress analysis to ensure that the design stress limits were not exceeded. The mechanical design is shown in Fig. 4. As shown, each ceramic segment is contoured to fit into a groove in the vane support and then pass under the trailing edge to butt against the adjacent segment. A cold gap of 0.020 in. was provided between the ceramic segments and the vane support to ensure that differential thermal expansion would not result in binding of the ceramic at operating temperatures. Analysis indicated that the gap would be reduced to approximately 0.009 in. at operating temperatures.

As shown in Fig. 4, the endwall is retained by two tangs extending from the pressure and suction walls of the airfoil. These tangs are cooled to approximately 1800°F by holes drilled into the vane cavity. The holes are drilled at an angle to prevent cooling air from impinging on the ceramic and producing high thermal gradients. The tang cooling is the only cooling required for the endwall and amounts to less than 50% of the coolant that would be required with a metal endwall. The design was analyzed using the latest three-dimensional heat transfer and stress analysis computer programs. The program divided the segment into 653 elements with eight nodes in each element, resulting in approximately 4200 unknowns for the stress analysis. Computer running time was 1 hr 15 min for each steady-state case calculated. The manner in which the segment was divided is shown in Figs. 5, 6, and 7.

The film temperature boundary conditions for the hot gas side of the ceramic endwall are shown in Fig. 8 and correspond to a gas stream at 2800°F and 200 psia. The boundary conditions reflect the effects of transition duct cooling air which was needed to cool the inlet to the test cascade and which is not untypical of a real engine environment. The hot gas side heat transfer coefficients were mapped using the technique described by M. F. Blair.[1] Under engine conditions approximately 1000°F air is used for coolant. The rig was limited to 200°F air and then a special artifice was required to simulate temperature gradients in the ceramic. A layer of insulating material was placed on the endwall to insulate the endwall from the coolant. The analysis and initial testing was carried out under this condition.

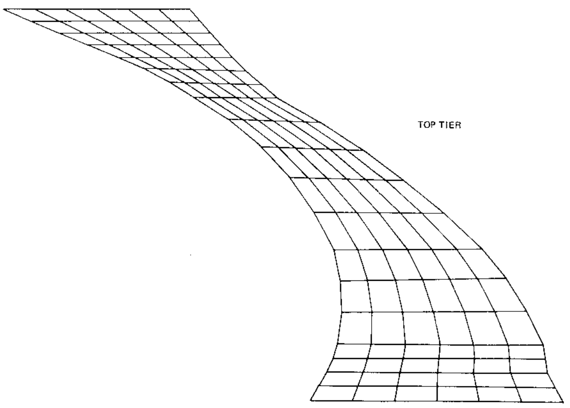

Fig. 6 **Top tier of ceramic endwall computer analysis break up.**

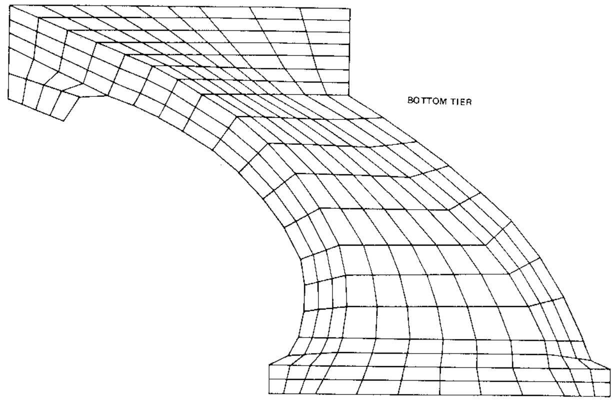

Fig. 7 **Bottom tier of ceramic endwall computer analysis break up.**

The heat transfer analysis involved both steady-state and transient conditions. The transient cycle simulated an engine deceleration from sea-level takeoff conditions to idle in 13 sec followed by an acceleration to sea-level takeoff conditions in 12 sec with 3 min for stabilization, as shown in Fig. 9. The results indicated that the maximum steady-state temperature at simulated sea-level takeoff conditions would be 2278°F and would occur near the airfoil gage section (the throat of the cascade). The minimum ceramic temperature would be 1807°F and would occur at the leading edge of the endwall segment. The overall average temperature was predicted to be 2095°F. The transient stress analysis was run for five points during the thermal transient. Because of the large amount of data produced by the analysis, the results were reduced to show only the maximum stress and strain for each of the five conditions during the transient. The results shown in Fig. 10 are for the point of maximum transient strain on the endwall. It occurs during deceleration and amounts to 0.0005 in./in., which is below the allowable strain.

The results for steady-state stress analysis are summarized in Figs. 11, 12, and 13 for sea-level static takeoff conditions. Again, because of the large quantity of data produced by the analysis, the results have been reduced to show only the more significant stresses. All other stresses are well below those indicated. The maximum steady-state stress was predicted to be 14.5 ksi and to occur at the trailing edge where the temperature is 2200°F. At this temperature, 14.5 ksi is 69% of the maximum allowable design stress. The region surrounding the location of the maximum stress is subjected to substantially lower stresses with the result that extensive stress redistribution will

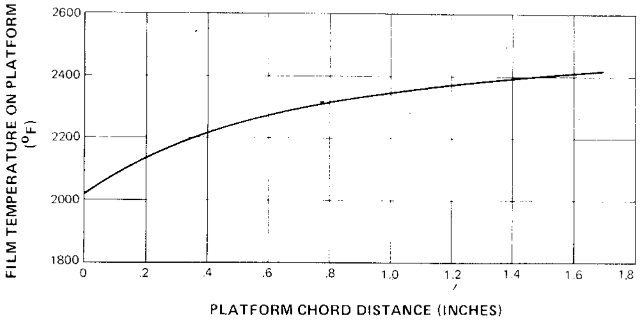

Fig. 8 **Film temperature boundary conditions for hot side of ceramic endwall.**

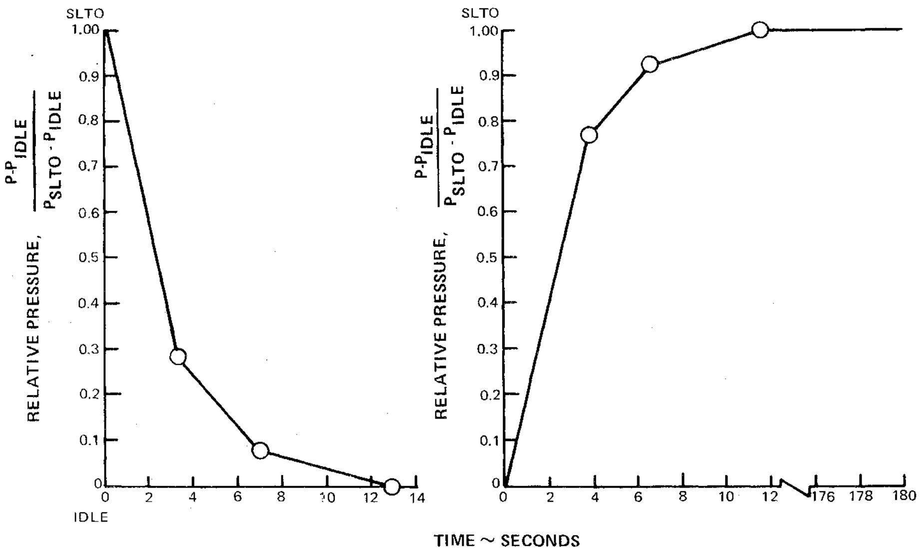

Fig. 9 Transient cycle assumed for heat transfer and stress analysis.

occur with time. The average stress for this region was predicted to be 6.3 ksi at 2200°F. The Larson-Miller plot for silicon nitride indicates that this stress would allow a creep life in excess of 400 hr based on the 60% design criterion.

Fabrication

The endwalls were produced by diamond grinding using metal-bonded diamond wheels with a grit no coarser than 220. Grinding was conducted with a wheel speed of 5000 surface ft/min with aqueous-base coolants. To simplify machining, the endwalls were formed as two intersecting flat planes rather than the more complicated curve that would normally be used. Hence, the initial machining operation consisted of grinding the ceramic material to the basic dihedral shape, after which the lip which mates with the vane was produced by three-dimensional grinding. To ensure a good, non-interfering fit between these surfaces and the mating surfaces, the vane contours were milled on tracer-controlled machines using identical airfoil contour drawings.

Fillet radii and edge chamfer for the endwalls were as generous as possible to avoid stress concentrations while still being consistent with design and tolerance requirements. Edge chamfers ranged from 0.015–0.025 in., while the fillet radii ranged from 0.050–0.080 in. Where possible, finish grinding was conducted parallel to the edges and the known principal stress directions. Following finish machining, the endwalls were subjected to detailed dimensional inspection, radiographic inspection, and to fluorescent penetrant inspection to detect any surface defects.

Test Program and Results

Three series of tests were conducted. The first involved thermal mapping to verify the heat transfer analysis, the second involved steady-state endurance testing to verify that the consequent steady-state stresses did not exceed the material capabilities, and the third consisted of thermal cyclic testing to determine the effects of thermal cyclic stresses. All testing was conducted in an annular segment cascade with six vanes. Initial testing was conducted with a single ceramic endwall, and all subsequent testing was conducted with three ceramic endwalls. The other endwalls and the six vanes in the cascade were transpiration-cooled metal parts.

Thermal Mapping

Temperature measurements for thermal mapping of the ceramic endwall surface temperatures were made with thermocouples, temperature-sensitive paint, and an optical pyrometer. The best results were obtained with the optical pyrometer, which provided reliable operation and good coverage over the complete endwall except for a small section near the trailing edge. Only limited data

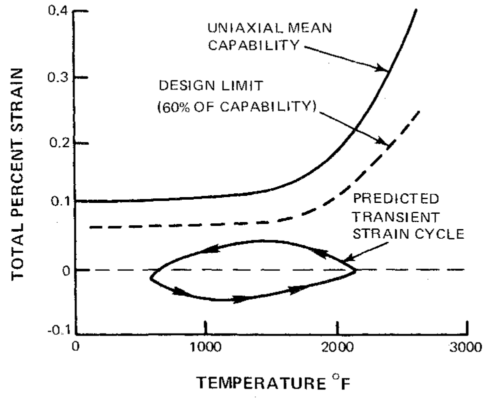

Fig. 10 Predicted maximum thermal strain for ceramic endwall.

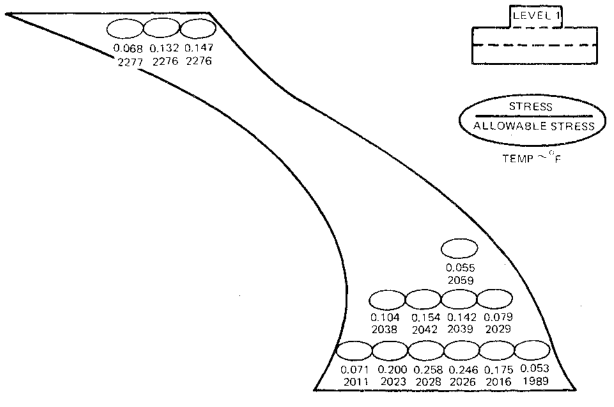

Fig. 11 Steady-state stress analysis results for top tier of ceramic endwall.

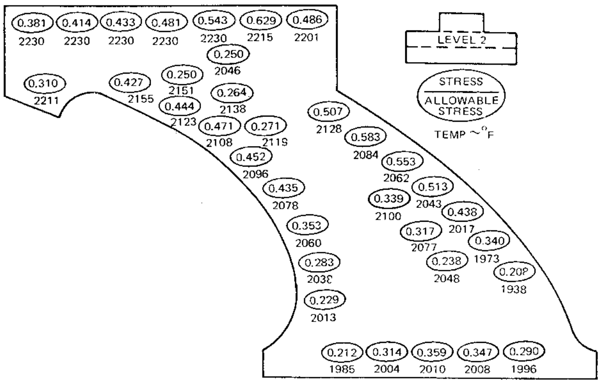

Fig. 12 Steady-state stress analysis results for middle tier of ceramic endwall.

was obtained from the thermocouples because of their poor durability, and the temperature sensitive paints proved unsatisfactory because of their poor adhesion to the ceramic.

The initial thermal mapping results indicated that the ceramic surface temperature was lower than desired for an accurate simulation of advanced engine conditions. These conditions resulted from the quantity and distribution of the transition duct coolant flow and the vane cooling flow. To improve the temperature simulation, the vanes were moved 0.15 in. into the gas stream, producing a small step to break up the coolant film, selected coolant air supply holes were sealed, and insulation was added under the endwalls. These modifications were successful in establishing the desired temperature pattern. The improvement can be seen in Fig. 14 by comparing the temperatures obtained in Run 2A near the beginning of the thermal mapping program and those obtained in Run 2D at the end of the program. It must be noted that this temperature pattern was not the same pattern which was used for the endwall stress analysis. The initial temperature pattern was predicted on the utilization of insulation on the non-gas path side of the endwall to simulate 1000°F cooling air. All attempts to install this insulation were unsuccessful, but insulation was installed in the vane platform region to help control the influence of the 200°F cooling air. Although the temperature level was somewhat lower than desired, stresses produced by thermal gradients during the test program were felt to be at least as severe as those predicted.

At the completion of the thermal mapping program, three ceramic endwalls were found to be damaged, as shown in Fig. 15. To determine the cause of the failures, a heat transfer analysis was conducted on the basis of the thermal mapping state to calculate the temperatures in the trailing edge region where optical pyrometer temperature readings could not be obtained. The results from this analysis indicated that high thermal gradients existed, although the consequent stresses were not above the material failure stress. Detailed dimensional analysis, however, revealed that repositioning the vanes and endwalls to a smaller diameter in the cascade to project the endwalls into the gas stream reduced the clearance between the vanes sufficiently that the vanes bound the endwalls at operating temperatures. The resulting stress in combination with the thermal stress appeared to be sufficient to cause the endwall failures. Consequently, the clearance between the endwalls and the vanes was increased by 0.020 in. in preparation for steady-state endurance testing.

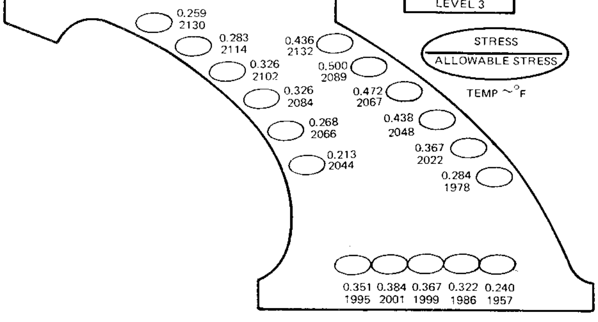

Fig. 13 Steady-state stress analysis results for bottom tier of ceramic endwall.

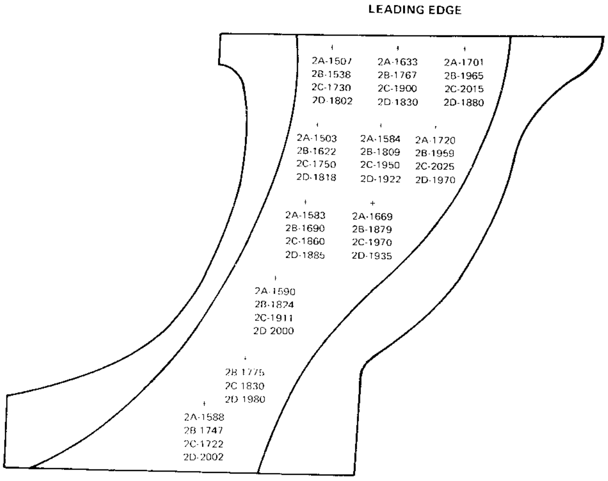

Fig. 14 Optical pyrometer temperature data for ceramic endwall during thermal mapping test. (Numbers indicate temperatures in °F.)

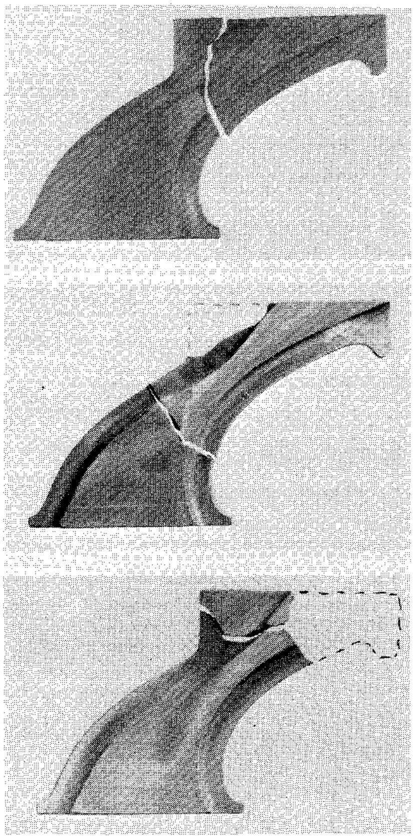

Fig. 15 Condition of ceramic endwalls following thermal mapping test.

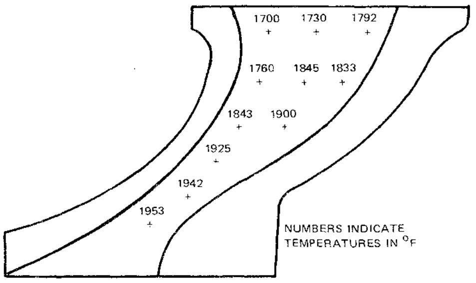

Fig. 16 Optical pyrometer temperature data for ceramic endwall during endurance test.

Steady State Endurance Test

Steady-state endurance testing was conducted with a gas stream temperature of 3000°F and a pressure of 200 psia. A total of 10.29 hr was accumulated, including six rapid cooling cycles simulating snap engine decelerations. All of the endwalls were in excellent condition at the end of the test. The temperatures indicated by optical pyrometer measurements at maximum test conditions are shown in Fig. 16. The good condition of the endwalls at the conclusion of this test verified that the binding between the vanes and the endwalls during thermal mapping was in fact the cause of the failures experienced during that test, since the increased clearance was sufficient to preclude failure. The six rapid deceleration thermal cycles completed in the course of the test provided a preliminary indication of the thermal cycle capability of the endwalls. Although acceleration was conducted slowly, deceleration involved a rapid transient and, according to the heat transfer analysis, should have produced the maximum thermal stress anticipated during the program. It is felt that, even though the analysis was conducted with a different endwall temperature pattern, the maximum thermal stress would still occur during the deceleration portion of the cycle.

Thermal Cyclic Endurance Testing

The thermal cyclic endurance test was conducted by cycling the gas stream temperature between 750°F, simulating idle engine conditions, and 3000°F at a pressure of 200 psia, simulating maximum engine conditions. A 6 min cycle was used with 3 min at each temperature. At the end of 23 cycles, the cascade was inspected, and two of the three endwalls were found to be damaged at the trailing edge. This damage was sufficiently minor that testing could have been continued, as shown in Fig. 17. However, the vanes and the metal transpiration-cooled endwalls were severely damaged, as shown in Fig. 18, requiring termination of the test.

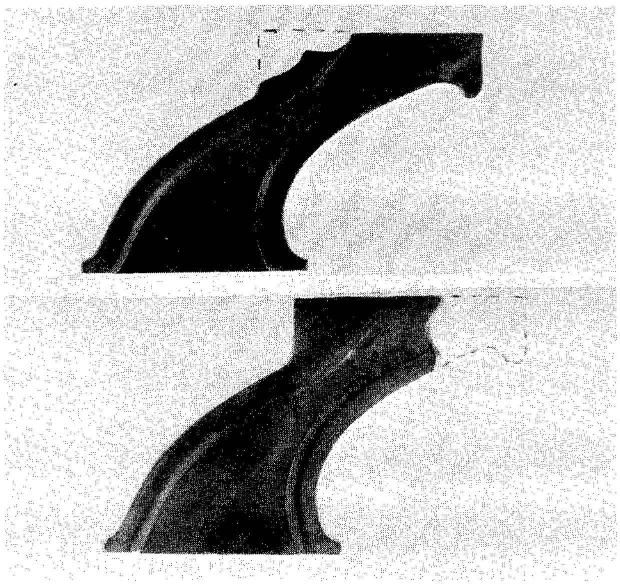

Fig. 17 Condition of ceramic endwalls following cyclic endurance test.

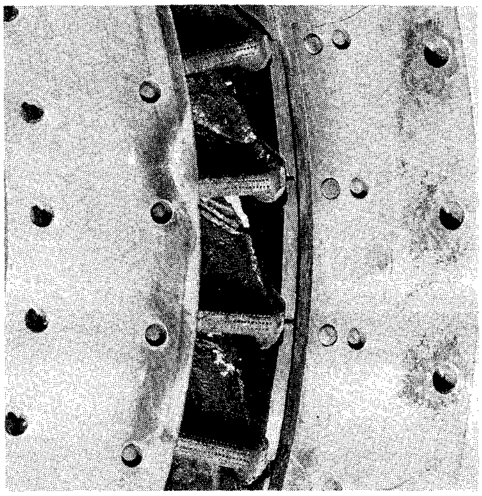

Fig. 18 Condition of transpiration-cooled turbine vanes following cyclic endurance test.

The fact that one of the ceramic endwalls remained in good condition throughout the test indicated the inherent capability of ceramic for endwall applications in advanced turbines. Further, since all of the endwalls had been subjected to rapid thermal cooling during the steady-state endurance test and had sustained no damage, it appears that the stresses causing trailing edge damage must have been induced during the acceleration portion of the cycle. Although these facts are not sufficient to positively identify the cause of the trailing-edge damage, mechanical binding is suspected to be a contributing cause.

Conclusions

The test program clearly demonstrated that ceramic technology has reached the level where ceramic endwalls could be developed for engine use. The program specifically demonstrated that ceramic endwalls can withstand the temperature and pressure loads produced in an advanced turbine operating with a gas stream temperature of 3000°F and a pressure of 200 psia. The program also demonstrated that the ceramic will withstand the thermal transient stresses induced during engine deceleration, which heat transfer and stress analysis indicate are the highest stresses to which the endwalls would be subjected in an engine.

The brittleness of the ceramic material will clearly require special design considerations since fracture, rather than local yielding, is the consequence of localized overstress. Consequently, adequate clearances are required to ensure that binding does not occur between the endwalls and the supports. The effect of these clearances and the associated leakage on turbine performance must be weighed against the improvement obtained through reduced cooling requirements in assessing the benefits of ceramic endwalls.

References

[1] Blair, M. F., "An Experimental Study of Heat Transfer and Film Cooling on Large-Scale Turbine Endwalls," ASME Paper 74-GT-35, *Journal of Heat Transfer,* Nov. 1974, pp. 524–529.